

gradients in order to check the validity of Eq. (13) for these cases as well.

Acknowledgment

The authors would like to thank the Deutsche Forschungsgemeinschaft (DFG) for supporting the work described in this paper.

References

- ¹Coles, D. E., "The Law of the Wake in the Turbulent Boundary Layer," *Journal of Fluid Mechanics*, Vol. 1, Feb. 1956, pp. 191–226.
- ²Pohlhausen, K., "Zur näherungsweisen Integration der Differentialgleichung der laminaren Reibungsschicht," *Zeitung für angewandte Mathematik und Mechanik*, Vol. 1, June 1921, pp. 252–268.
- ³Coles, D. E. and Hirst, E. A., "Computation of the Turbulent Boundary Layers," *Proceedings of the 1968 AFOSR-IFP-Stanford Conference*, Vol. II, Compiled Data, Stanford Univ., Stanford, CA, 1969.
- ⁴Pfeil, H. and Stickse, W. J., "Influence of the Pressure Gradient on the Law of the Wall," *AIAA Journal*, Vol. 20, March 1982, pp. 434–436.
- ⁵Nikuradse, J., "Gesetzmäßigkeiten der turbulenten Strömung in glatten Röhren," *VDI-Forschungsheft* 356, Vol. 3, Sept. 1932.
- ⁶Coantic, M., "Contributions à l'étude de la structure de la turbulence dans une conduite circulaire," Dissertation, University d'Aix-Marseille, France, 1966.
- ⁷Hinze, J.O., *Turbulence*, McGraw-Hill, New York, 1959.
- ⁸Falkner, V. M. and Skan S. W., Solution of the Boundary Layer Equations," *The London Edinburgh and Dublin Philosophical Magazine and Journal of Science* 7th Ser., Nov. 1931, p. 865.
- ⁹Scönauer, W., "Ein Differenzenverfahren zur Lösung der Grenzschichtgleichungen für stationäre, laminare, inkompressible Strömung," *Ingenieurarchiv*, Vol. 33, June 1964, p. 173.
- ¹⁰Terrill, R. M., "Laminar Boundary-Layer Flow Near Separation With and Without Suction," Vol. 253, No. 1, 1960, p. 55.
- ¹¹Schubauer, G. B. and Klebanoff, P. S., "Contributions on the Mechanics of Boundary-Layer Transition," NACA Report 1289, Feb. 1955.
- ¹²Feindt, E. G., "Untersuchung über die Abhängigkeit des Umschlages laminar-turbulent von der Oberflächenrauigkeit und der Druckverteilung," Dissertation, TH Braunschweig, Institut für Strömungsmechanik, FRG, 1956.
- ¹³Schröder, T., "Entwicklung des instationären Nachlaufs hinter quer zur Strömungsrichtung bewegten Zylindern und dessen Einfluß auf das Umschlagverhalten von ebenen Grenzschichten stromabwärts angeordneter Versuchskörper," Dissertation, TH Darmstadt, Institut für Thermische Turbomaschinen, FRG, 1985.
- ¹⁴Erm, L. P., Smits, A. J., and Joubert, P. N., "Low Reynolds Number Turbulent Boundary Layers on a Smooth Flat Surface in a Zero Pressure Gradient," *Turbulent Shear Flow*, F. Durst, B. E. Launder, J. L. Lumley, F. W. Schmidt, and J. H. Whitelaw, Springer-Verlag, Berlin.
- ¹⁵Granville, P. S., "The Calculations of Viscous Drag of Bodies of Revolution," U.S. Navy, Report 849, 1953. David Taylor Model Basin.

Mass Transfer in a Binary Gas Jet

J. Y. Zhu,* R. M. C. So,† and M. V. Ötügen‡
Arizona State University, Tempe, Arizona

Introduction

TURBULENT gas jets have been investigated extensively in the past because of their intrinsic importance to the

study of supersonic and hypersonic flows, combustor performance, geophysical flows, and variable-density mixing phenomena. In most of the earlier investigations, measurements were limited to the jet growth rate, centerline decay behavior, and similarity scaling parameters.¹ With the advent of hot-wire anemometry, hot-wire type concentration probes were developed to measure the concentration field alone^{2,3} and to measure the concentration and velocity fields simultaneously.^{4,5} Later, these probes were used to study the density field in a two-dimensional mixing layer of helium and nitrogen³ and to measure velocity and helium volume concentration simultaneously in a helium/air mixture.⁵ The latter study was able to demonstrate that some of the turbulent mass flux terms normally neglected in the jet equations were not small compared to those mass flux terms that were retained in the equations. Since detailed measurements of the mixing process were not made, the behavior of mass transfer in a variable-density flow was not studied.

Alternatives to hot wires are optical techniques. Batt⁶ proposed the use of a fiber-optic probe to measure species concentration whereas Raman and Rayleigh scattering techniques were developed by Birch et al.⁷ and Pitts and Kashiwagi.⁸ These techniques were far better than the hot-wire probe⁴ because the concentration measurements were independent of velocity, and they can be integrated easily with laser Doppler anemometry (LDA) to measure concentration simultaneously with velocity. Even though LDA/Raman and LDA/Rayleigh techniques have not been used to study binary mixing, the two techniques have been applied to examine premixed^{9,10} and nonpremixed¹¹ flames. These studies led to an understanding of mass transfer in flames and showed that, because of heat-release effects, the gradient diffusion assumption that was commonly made to model turbulent axial mass flux was not valid.¹¹ In spite of these advances, mass transfer in isothermal, binary mixing is still little understood.

Since the hot-wire type concentration probe² measures species concentration independent of upstream velocity, it can be used with LDA to measure velocity and concentration simultaneously. Zhu et al.¹² took advantage of this fact and developed a laser/hot-wire technique to do just that. As a result, a simple technique is now available for the study of mass transfer in binary gas jets. This Note presents the results of an attempt to use the laser/hot-wire technique¹² to measure velocity and concentration simultaneously in the developing region of a free binary gas jet.

Experimental Setup

The jet test rig consisted of a cylindrical plenum fitted with a well-contoured convergent nozzle at one end of the cylinder. The cylindrical plenum was 304.8 mm in depth and 132.4 mm in diameter, while the jet nozzle diameter (D) was 9.5 mm. A honeycomb section of 127 mm in length installed just ahead of the convergent nozzle was used to straighten the flow and to destroy the large eddies inside the plenum. Premixed helium/air mixture with 50% of helium by volume was delivered to the plenum from compressed gas bottles. A DISA Model 55L18 seeding generator capable of generating liquid droplets (50% water and 50% glycerine), centered around 1 μ m in size, was connected to the plenum. Since the liquid droplets were carried into the plenum by an air stream, the resultant helium/air mixture delivered to the jet had a helium volume concentration of <50% depending on the droplet concentration required for accurate LDA measurements of the jet velocity field. Once the right droplet concentration was determined, the supply pressures of the seeding generator air stream and the helium/air mixture were fixed and maintained constant for the whole experiment. Consequently, a fairly constant jet plenum condition was obtained, and the jet velocity and helium volume concentration were quite uniform at the jet nozzle exit. The whole facility was arranged vertically so

Received Jan. 4, 1988; revision received May 6, 1988; presented as Paper 88-3813 at the 1st National Fluid Dynamics Congress, Cincinnati, OH, July 25–28, 1988. Copyright © 1988 by Ronald So. Published by the American Institute of Aeronautics and Astronautics, Inc., with permission.

*Graduate Assistant, Mechanical and Aerospace Engineering Department.

†Professor, Mechanical and Aerospace Engineering Department.

‡Research Associate, Mechanical and Aerospace Engineering Department.

that a free round jet in the vertical direction was established. This was necessary in order to eliminate buoyancy effects across the jet.

The laser/hot-wire measurement technique of Zhu et al.¹² was used to measure the jet flow. Details of the technique and the various instruments used are given in Ref. 12. The LDA and the concentration probe were mounted on a two-dimensional manual traversing mechanism. Traverse in the radial or r direction was accurate to 0.2 mm whereas in the axial or x direction was accurate to 0.5 mm. However, the spatial resolution of the setup was determined by the LDA sampling volume that has dimensions of about 1 mm length and 0.06 mm width, and the location of the concentration probe, which was set up at about 0.5 mm behind the sampling volume. Once the probe was properly installed, the whole setup was fixed and the traverses were controlled by the two-dimensional traversing mechanism. The LDA system was first set up to measure \tilde{u} , the instantaneous axial velocity. This, together with the concentration probe, gave simultaneous measurements of \tilde{u} and \tilde{c} , the instantaneous helium volume concentration. Then, the optics in the LDA system were rotated by $\pi/2$ to facilitate the measurements of \tilde{v} , the instantaneous radial velocity. Since $\tilde{\theta}$ and $\tilde{\rho}$ are related to \tilde{c} , the signals were analyzed to give the statistics of \tilde{u} , \tilde{v} , \tilde{c} , $\tilde{\theta}$, $\tilde{\rho}$, $\rho'u'$, and $\rho'v'$, where $\tilde{\theta}$ and $\tilde{\rho}$ are the instantaneous mixture mass fraction and density, respectively, and the prime quantities represent the fluctuating components. The sampling rate was always chosen to be much less (roughly an order of magnitude) than the particle arrival rate in order to avoid bias in the velocity measurements.¹³ Consequently, the velocity data were sampled at fairly low rates and spectral calculations were not attempted.

Discussion of Results

As the jet grows, the cross-sectional area increases and the seeding concentration decreases. Therefore, the LDA signal will become weaker as the traverse moves downstream and towards the edge of the jet. Consequently, simultaneous measurements of \tilde{u} , \tilde{v} , and \tilde{c} were carried out only at the following locations: $x/D=0.46$, 3.80, 5.13, 6.46, and 9.13. The jet Reynolds number was determined to be 4300, and the jet-to-ambient fluid density ratio was 0.64.

Results of the measurements at $x/D=0.46$ are presented in Fig. 1. The mean axial velocity and mixture fraction, U and θ , are indeed uniform over 90% of the jet nozzle diameter, and the jet boundary does not show any appreciable growth at this point. This shows that the flow at the jet exit is axisymmetric and very uniform and the turbulence level is low, approximately 1% for \tilde{u} and $\tilde{\theta}$ and 2% for \tilde{v} . However, the turbulent mass fluxes across the jet are not uniform. The flux $-\rho'v'$ is positive all across the jet, while the flux $-\rho'u'$ is negative. Scatter in $-\rho'u'$ and $-\rho'v'$ is large because of the large measuring volume. Even then, a clear trend is evident in the measurements of $-\rho'v'$ and $\rho'u'$. The flux $-\rho'v'$ increases as the jet edge is approached, while the flux $-\rho'u'$ decreases away from the jet centerline. Since θ , and hence ρ (the mean mixture density), is constant across the jet, the gradient diffusion relation

$$-\overline{\rho'v'} = D_T \frac{\partial \rho}{\partial r} \quad (1)$$

is not valid in the region immediately downstream of the jet exit, where D_T is the turbulent diffusivity. It is not possible to comment on the relation

$$-\overline{\rho'u'} = D_T \frac{\partial \rho}{\partial x} \quad (2)$$

because $\partial \rho / \partial x$ at this location is not known. The results suggest that $\partial \rho / \partial x$ is zero at the centerline but becomes negative as r increases.

In order to assess the gradient diffusion relations, Eqs. (1) and (2), in the developing region of the jet, the mean density gradients $\partial \rho / \partial r$ and $\partial \rho / \partial x$ also were calculated from the measured data. These are plotted with $\rho'u'$ and $\rho'v'$ in Figs. 2 and 3. If Eqs. (1) and (2) are valid, $\rho'v'$ and $\partial \rho / \partial r$ are of opposite sign and so are $\rho'u'$ and $\partial \rho / \partial x$. The results shown in Fig. 2 validate the gradient diffusion relation, Eq. (2), for $\rho'u'$ at $x/D \geq 6.46$. For smaller x/D , Eq. (2) is not valid over a

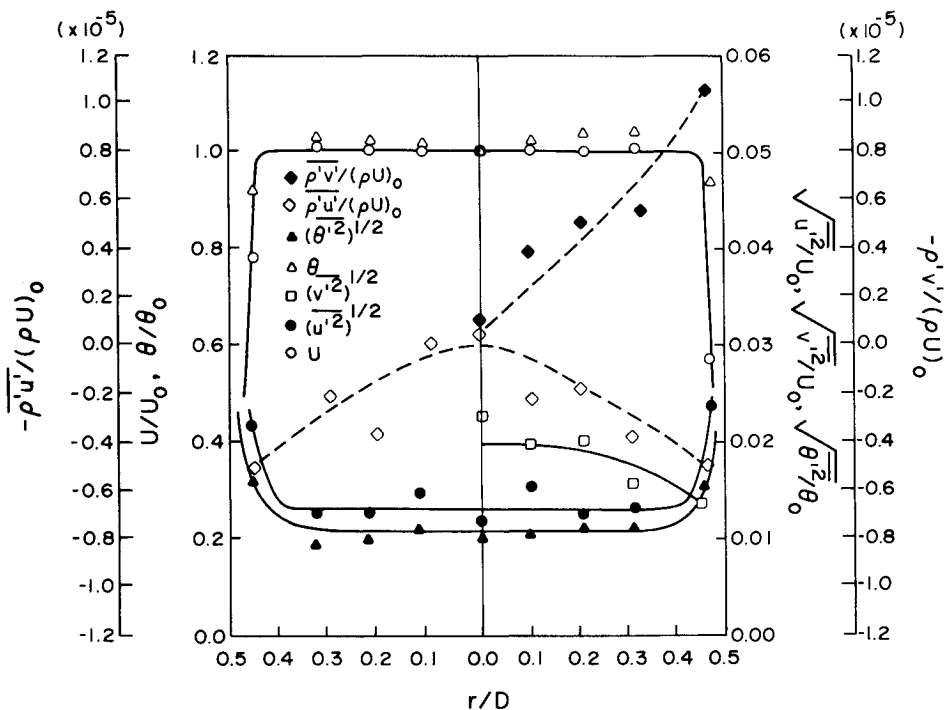


Fig. 1 Properties of jet at $x/D=0.46$.

substantial part of the jet, except near the jet core where $\overline{\rho'u'}$ and $\partial\rho/\partial x$ are of opposite sign. On the other hand, the gradient diffusion relation, Eq. (1), is valid for $\overline{\rho'u'}$ downstream of $x/D=5.13$. At $x/D=3.8$, Eq. (1) is not valid inside the jet potential core but is true over the rest of the jet region. This behavior is opposite to that of $\overline{\rho'u'}$ and points to the difficulty of modeling the near field of a binary gas jet through the gradient diffusion assumption. These results show that the jet adjusts slowly to a gradient transport process. From the measured $\overline{\rho'u'}$ and $\overline{\rho'v'}$, it is obvious that D_T is not constant across the jet. This finding is consistent with the theoretical result of So and Liu.¹⁴

Both $\overline{\rho'u'}$ and $\overline{\rho'v'}$ are two orders of magnitude larger than their corresponding values at $x/D=0.46$ and show their rapid increase in the jet near field. The mass flux profiles show one peak in the mixing region of the jet. As the jet develops, the peak value decreases, rather drastically for $\overline{\rho'v'}$ but not as drastic for $\overline{\rho'u'}$. The eventual peak value reached by $\overline{\rho'u'}$ and $\overline{\rho'v'}$ is about the same. In general, $\overline{\rho'u'}$ and $\overline{\rho'v'}$ are about equal across the jet and so are their variations with r and x . This means that the axial gradients of $\overline{\rho'u'}$ and $\overline{\rho'v'}$ are about equal and so are their respective radial gradients.

If the jet Reynolds number is very high, viscous effects can be neglected, then the Reynolds equations for isothermal, binary gas jets can be simplified to those given by So and Liu.¹⁴ The simplified equations may be true for the jet far field.¹⁴ However, the validity of the simplified equations for the jet near field has not been sufficiently demonstrated. The present results show that, in the jet near field, the terms $\overline{\rho'v'U}$, $\overline{\rho'u'V}$, $\overline{\rho'v'V}$, and $\overline{\rho'u'U}$ are not small compared to $\overline{\rho'u'v'}$. Consequently, the resultant jet equations are different from those given by So and Liu¹⁴ because diffusion in the x direction is also significant in the jet near field. Therefore, the present results cast doubt on the suitability of the conventional jet equations for the jet near field because neglecting the turbulent mass flux terms in the jet near field may not be justified.

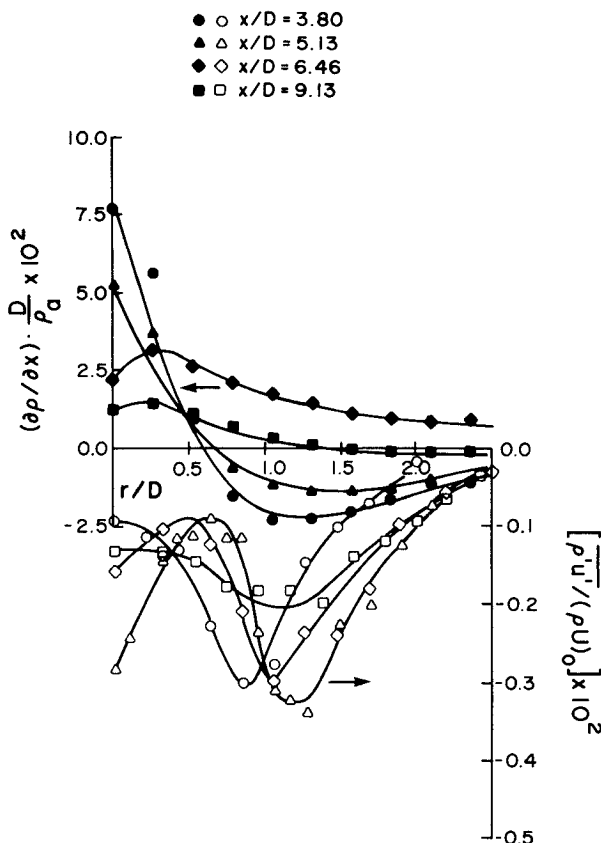


Fig. 2 Distributions of $\overline{\rho'v'}$ and $\partial p/\partial x$ across the jet.

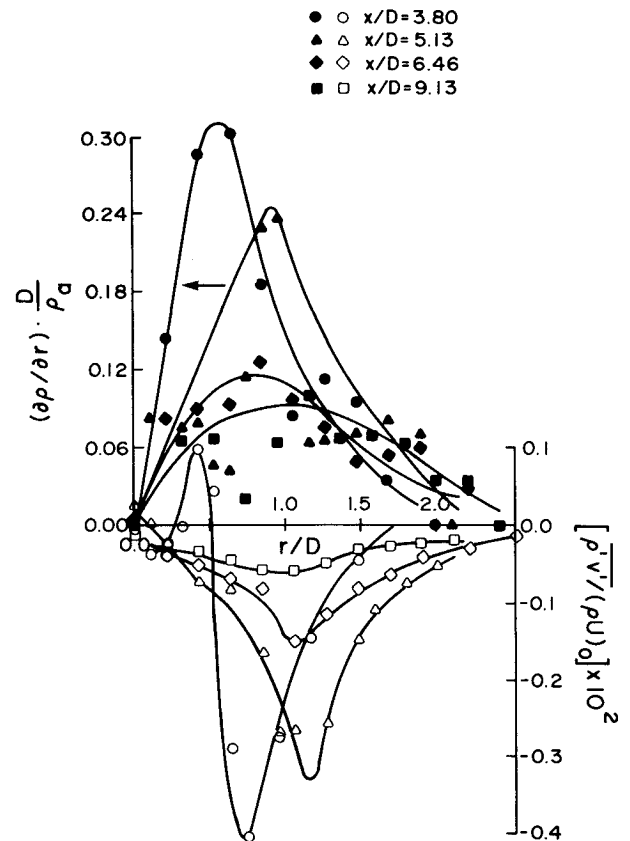


Fig. 3 Distributions of $\overline{\rho'u'}$ and $\partial p/\partial r$ across the jet.

Acknowledgment

This research was conducted under Contract N6053085-C-9001 funded by Naval Weapons Center, China Lake, CA 93555.

References

- ¹Abramovich, G. N., Yakovlevsky, O. V., Smirnova, I. P., Secundov, A. N., and Krasheninnikov, S. Yu., "An Investigation of the Turbulent Jets of Different Gases in a General Stream," *Acta Astronautica*, Vol. 14, 1969, pp. 229-240.
- ²Brown, G. L. and Rebollo, M. R., "A Small Fast-Response Probe to Measure Composition of a Binary Gas Mixture," *AIAA Journal*, Vol. 10, 1972, pp. 649-652.
- ³Brown, G. L. and Roshko, A., "On Density Effects and Large Structure in Turbulent Mixing Layers," *Journal of Fluid Mechanics*, Vol. 64, 1974, pp. 775-816.
- ⁴Way, J. and Libby, P. A., "Hot-Wire Probes for Measuring Velocity and Concentration in Helium-Air Mixtures," *AIAA Journal*, Vol. 8, 1970, pp. 976-978.
- ⁵Stanford, R. A. and Libby, P. A., "Further Applications of Hot-Wire Anemometry to Turbulence Measurements in Helium-Air Mixtures," *Physics of Fluids*, Vol. 17, 1974, pp. 1353-1361.
- ⁶Batt, R. G., "Turbulent Mixing of Passive and Chemically Reacting Species in a Low-Speed Shear Layer," *Journal of Fluid Mechanics*, Vol. 82, 1977, pp. 53-95.
- ⁷Birch, A. D., Brown, D. R., Dodson, G. M., and Thomas, J. R., "The Turbulent Concentration Field of a Methane Jet," *Journal of Fluid Mechanics*, vol. 88, 1978, pp. 431-449.
- ⁸Pitts, W. M. and Kashiwagi, T., "The Application of Laser-Induced Rayleigh Light Scattering to the Study of Turbulent Mixing," *Journal of Fluid Mechanics*, Vol. 141, 1984, pp. 391-429.
- ⁹Moss, J. B., "Simultaneous Measurements of Concentration and Velocity in an Open Turbulent Flame," *Combustion Science and Technology*, Vol. 22, 1980, pp. 119-129.
- ¹⁰Heiler, M. V., Taylor, A. M. K. P., and Whitlaw, J. H., "Simultaneous Velocity and Temperature Measurements in a Premixed

Flame," *Experimental Fluids*, Vol. 3, 1985, pp. 323-339.

¹¹Driscoll, J. F., Schefer, R. W., and Dibble, R. W., "Mass Fluxes $\rho'u'$, and $\rho'v'$, measured in a Turbulent Nonpremixed Flame," *Proceedings of the Nineteenth Symposium (International) on Combustion*, The Combustion Inst., Pittsburgh, PA, 1982, pp. 477-485.

¹²Zhu, J. Y., So, R. M. C., and Otugen, M. V., "Turbulent Mass Flux Measurements Using a Laser/Hot-Wire Technique," *International Journal of Heat and Mass Transfer*, Vol. 31, 1988, pp. 819-829.

¹³Stevenson, W. H., Thompson, H. D., and Roesder, T. C., "Direct Measurement of Laser Velocimeter Bias Errors in a Turbulent Flow," *ALAA Journal*, Vol. 20, 1982, pp. 1720-1723.

¹⁴So, R. M. C. and Liu, T. M., "On Self-Preserving, Variable-Density Turbulent Free Jets," *Zeitschrift für angewandte Mathematik und Physik*, Vol. 37, 1986, pp. 538-558.

Unsteady Transition Location

Kenneth F. Stetson*

Air Force Wright Aeronautical Laboratories,
Wright-Patterson Air Force Base, Ohio

Nomenclature

h	= local heat transfer coefficient (recovery temperature of $0.9 T_0$ assumed, Btu/ft ² -s °R)
k	= roughness height, cm (in.)
p	= pressure, k Pa (lb/in. ²)
R	= radius, cm (in.)
Re	= Reynolds number
Re_{x_T}	= transition Reynolds number based upon conditions at the edge of the boundary layer and the surface distance from the stagnation point to the location of transition
Re_θ	= Reynolds number based upon conditions at the edge of the boundary layer and the laminar boundary-layer momentum thickness
t	= time, s
T	= temperature, °K(°R)
X	= surface distance, cm (in.)
θ	= laminar boundary-layer momentum thickness, cm (in.)

Subscripts

ad	= adiabatic
B	= base
e	= edge of boundary layer
N	= nose
w	= wall
∞	= freestream

Received Oct. 20, 1987. This paper is declared a work of the U.S. Government and is not subject to copyright protection in the United States.

*Aerospace Engineer, High Speed Aero Performance Branch, Aeromechanics Division, Flight Dynamics Laboratory. Associate Fellow AIAA.

Introduction

THE movement of boundary-layer transition on a wind tunnel model, while the freestream conditions remain constant, is an old topic, yet one that is not well understood. The stability theory of Lees¹ indicated that wall cooling had a stabilizing effect on a laminar boundary layer at supersonic Mach numbers. Van Driest² made calculations that indicated after a certain cooling temperature ratio was exceeded, the boundary layer remained laminar for any Reynolds number. Subsequently, wind tunnel experiments were performed to check the validity of these theoretical predictions. The early wind tunnel investigations of the effect of wall cooling on boundary-layer transition found, as predicted by theory, that decreasing the model surface temperature increased the transition Reynolds number. However, when liquid nitrogen was used to obtain additional surface cooling, an unexpected event occurred³: The stabilizing trend was reversed and the transition Reynolds number decreased with further reductions in surface temperature. There were two branches of the Re_{x_T} vs T_w/T_{ad} curve: The upper branch followed the trend of theory and suggested that the laminar boundary layer would be completely stabilized for temperature ratios below about 0.5; the lower branch showed an adverse effect of surface cooling that has never been explained (called transition reversal). Transition reversal was observed for several configurations, both with and without surface roughness. Surface roughness was not believed to provide a suitable answer for the observed results.

Muir and Trujillo⁴ reported an unsteady transition location on their blunt 8-deg half-angle cone tested at Mach 6. They observed that for the 32% blunt nosetip ($R_N/R_B = 0.32$), transition moved rearward with time, similar to the blunt configurations of Ref. 3. It was noted that this phenomenon occurred only with the large nosetip bluntness, and for the sharper configurations, which were subjected to the same environment and experienced similar increases in wall temperature, the transition location remained unchanged with time.

During the course of a more recent wind tunnel investigation of the effects of nosetip bluntness on boundary-layer transition, some transition movement with time results were also obtained.⁵⁻⁷ These new results do not provide an explanation for the transition-reversal phenomenon, but they do provide a better understanding of why transition can be unsteady on some blunt configurations.

Results and Discussion

The experiments were conducted in the Flight Dynamics Laboratory Mach 6 wind tunnel. This tunnel is a blow-down facility operating at a reservoir temperature of 611 K (1100°R) and a reservoir pressure range of 4827 to 14,480 k Pa (700 to 2100 psia), corresponding to a unit Reynolds number range of 31.8×10^6 to $99.4 \times 10^6/\text{m}$ (9.7×10^6 to $30.3 \times 10^6/\text{ft}$). The test core of approximately 25.4 cm (10 in.) is produced by a contoured axisymmetric nozzle with a physical exit diameter of 31.2 cm (12.3 in.). Additional details of the wind tunnel can be found in Ref. 8. The test model was a thin-skin, 8-deg half-angle cone containing two rays of thermocouples and had a base diameter of 10.2 cm (4 in.). The location of boundary-layer transition was obtained from heat-transfer measurements. Heat-transfer rates were calculated from the increase in the wall temperature of the model, using standard thin-skin data reduction techniques.

Transition experiments of Ref. 7 found low transition Reynolds numbers associated with the initial portion of a cone frustum; i.e., for several nose radii downstream from the nosetip, in spite of the existence of a favorable pressure gradient (designated as early frustum transition). It was determined that nosetip instabilities were responsible for these low transition Reynolds numbers and that the occurrence of transition in this region could be related to some threshold value of nosetip Reynolds number and nosetip roughness. This was the